Liquid Crystals
Publication details, including instructions for authors and subscription information:
http://www.informaworld.com/smpp/title~content=t713926090

Stable frustrated phases in chiral liquid crystals derived from optically active (*R*)- and (*S*)-3-ethylmercapto-2-methylpropionic acids

S. L. Wu[a]; J. H. You[a]; B. J. Uang[b]
[a] Department of Chemical Engineering, Tatung University, 40 Chunghan N. Rd., 3rd Sec., Taipei, Taiwan 104, ROC, [b] Department of Chemistry, National Tsinhua University, Hsinchu, Taiwan ROC,

Online publication date: 06 August 2010

To cite this Article Wu, S. L. , You, J. H. and Uang, B. J.(2001) 'Stable frustrated phases in chiral liquid crystals derived from optically active (*R*)- and (*S*)-3-ethylmercapto-2-methylpropionic acids', Liquid Crystals, 28: 1, 69 — 75
To link to this Article: DOI: 10.1080/02678290010003714
URL: http://dx.doi.org/10.1080/02678290010003714

LIQUID CRYSTALS, 2001, VOL. 28, NO. 1, 69–75

Stable frustrated phases in chiral liquid crystals derived from optically active (*R*)- and (*S*)-3-ethylmercapto-2-methylpropionic acids

S. L. WU*, J. H. YOU

Department of Chemical Engineering, Tatung University, 40 Chunghan N. Rd., 3rd Sec., Taipei, Taiwan 104, ROC

and B. J. UANG

Department of Chemistry, National Tsinhua University, Hsinchu, Taiwan ROC

(*Received 15 December 1999; in final form 10 July 2000; accepted 10 July 2000*)

Highly optically pure (*R*)- and (*S*)-3-ethylmercapto-2-methylpropionic acids were synthesized by using optically active (D)- and (L)-2,10-camphorsultams as chiral auxiliaries, respectively. Their derivatives, (*R*)- and (*S*)-EMMPN*m*B ($m = 6$–12), were prepared for investigation. Microscopic texture observations demonstrated that the materials possess three stable frustrated phases: BP, TGB_A^* and TGB_C^* phases. Interestingly, it was found that the N* phase behaves as an intermediary phase between BP and TGB_A^* phases in a rather narrow temperature range (calc. 0.5–1.4°C). A study of the racemic mixture, (±)-EMMPN*m*B ($m = 10$), indicated that the chirality of the molecule could suppress the formation of smectic phases in the heating process. An increase of alkyl chain length favoured the formation of the TGB phases particularly, in accompaniment with a change of TGB phases from monotropic to enantiotropic. Moderate maximum $\mathbf{P}_S$ values (calc. 14–19 nC cm^{-2}) and apparent tilt angle (calc. 20°) were obtained for the TGB_C^* phase in a surface stabilized ferroelectric liquid crystal geometry.

1. Introduction

Two kinds of frustrated phases, the blue phases (BPs) [1–4] and the twisted grain boundary (TGB) phases [5–10], have been of great interest in chiral liquid crystal systems for the past 10 years. Many compounds have been synthesized and investigated to account for the formation of these phases, and a general structure–property relationship has been established [11]. The results indicated that the molecules require high chirality and optical purity to generate these phases. Thus, the optically active chiral moieties used as chiral building blocks for the preparation of the chiral liquid crystals were generally optically active alkan-2-ols, lactic acid, and α-halohydrines derived from L-amino acids.

We have previously synthesized a series of chiral materials derived from highly optically pure (*R*)-3-ethylmercapto-2-methylpropionic acid, and found that the materials exhibit antiferroelectricity [12]. In this paper, we report a new series of chiral materials derived from the same chiral acids that exhibit mostly stable frustrated phases. This series, (*R*)- and (*S*)-6-(3-ethylmercapto-2-methylpropionyloxy)-2-naphthyl 4-alkoxybenzoates, EMMPN*m*B ($m = 6$–12), has the general formula shown below.

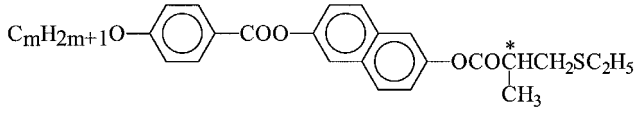

EMMPN*m*B (m=6-12)

2. Experimental

2.1. *Characterization of materials*

The purity of the target materials was estimated by thin layer chromatography and further confirmed by elemental analysis using a Perkin-Elmer 2400 spectrometer. The chemical structures of materials were analysed by proton magnetic resonance spectroscopy using a JEOL EX400 FT-NNM spectrometer. The magnitudes of specific rotation $[\alpha]_D$ were measured in anhydrous CH_2CI_2 using a JASCO DIP-360 digital polarimeter. Transition temperatures were determined by a DuPont DSC-910 calorimeter at a scanning rate of 1°C min^{-1}. Mesophases for the products were identified by observing

*Author for correspondence; e-mail: slwu@ttu.edu.tw

Liquid Crystals ISSN 0267-8292 print/ISSN 1366-5855 online © 2001 Taylor & Francis Ltd
http://www.tandf.co.uk/journals
DOI: 10.1080/02678290010003714

textures using a Nikon Microphot-FXA optical microscope under crossed polarizers, with a Mettler FP82-HT in connection with FP80 hot stage as a temperature controller. Homogeneously aligned cells of thickness 5 μm were purchased from Likam Scientific Instrument Limited Co., UK. In order to obtain a unit domain, a frequency alternation electric field (f = 50.5 Hz–2.5 kHz, E = 10.0–20 $V_{p\text{-}p}$, wave from triangular or square wave) was applied to the cells in the cooling process. The spontaneous polarization was measured by the triangular wave method [13] with a frequency of 100 Hz and amplitude 38.5 $V_{p\text{-}p}$. The apparent tilt angle was measured by the electric-optical method.

2.2. *Preparation of materials*

Tetrahydrofuran (THF), dichloromethane (CH_2Cl_2), benzene and pyridine were dried by treating with $LiAlH_4$, CaH_2, sodium and CaH_2, separately, and distilled before use. Optically active (*R*)-3-ethylmercapto-2-methylpropionic acid **5a** was prepared, by using (D)-2,10-camphorsultam **1** as a chiral auxiliary, according to the method described before [12]. The synthetic procedures are outlined in scheme 1. The sultam **1** was *N*-acylated by treatment with sodium hydride and the subsequent addition of methacryloyl chloride to obtain *N*-methacryloylsultam **2**. Michael addition of ethanethiol to *N*-methacryloylsultam **2** in the presence of *n*-butyllithium gave adducts **3** and **4**. Compound **3** obtained in pure form after recrystallization from CH_2Cl_2/*n*-hexane, was hydrolyzed with lithium hydroxide in aqueous tetrahydrofuran to give chiral acid **5a**. The enantiomeric compound (*S*)-3-ethylmercapto-2-methylpropionic acid **5b** was prepared in the same manner as for **5a** by using (L)-2,10-camphorsultam as a chiral auxiliary. Both chiral acids were purified by vacuum distillation. The optical purity of the enantiomeric acids was investigated by monitoring the hydrolytic reaction of compound **3** in deuteriated water solution and analysing the recovered acids using ^{1}H NMR spectroscopy [12]. The acids possessed high enantiomeric excess (≧98%) as expected.

The derivatives, (*R*)- and (*S*)-6-(3-ethylmercapto-2-methylpropionyloxy)-2-naphthyl 4-alkoxybenzoates, EMMPN*m*B (m = 6–12), were synthesized according to the procedures outlined in scheme 2. Alkoxybenzoic acids **6-m** were converted to acid chlorides **7-m** by reacting with oxalyl chloride. This was followed by the addition of acid chlorides **7-m** to excess amount of 2,6-dihydroxynaphthalene in the presence of pyridine to give alcohols **8-m**. Esterification of the alcohols **8-m** and chiral acids **5** by treatment with *N*,*N*′-dicyclohexylcarbodiimide (DCC) and 4-dimethylaninopyridine (DMAP) gave the target materials.

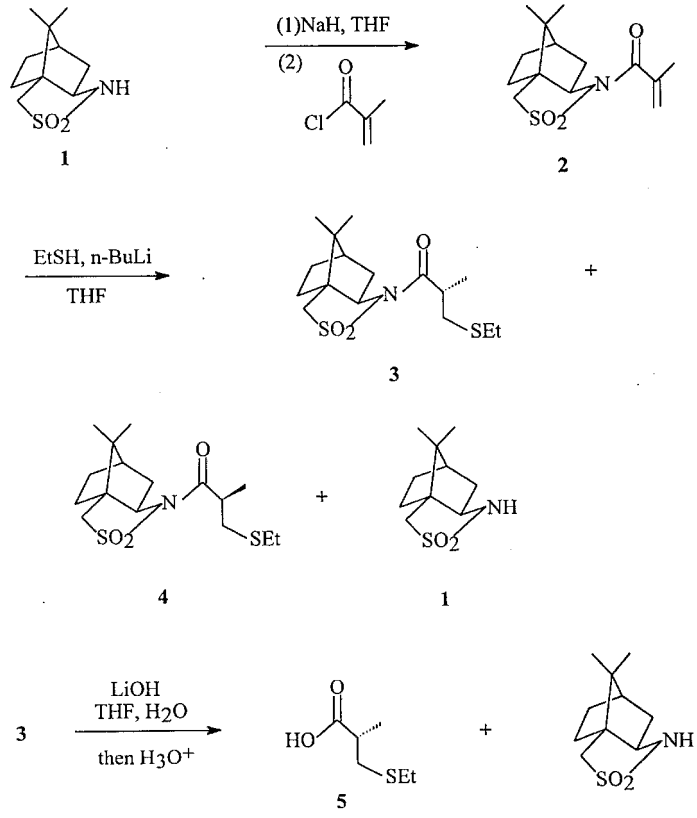

Scheme 1. The synthetic procedures for the chiral tails: (*R*)- and (*S*)-3-ethylmercapto-2-methylpropionic acids **5**.

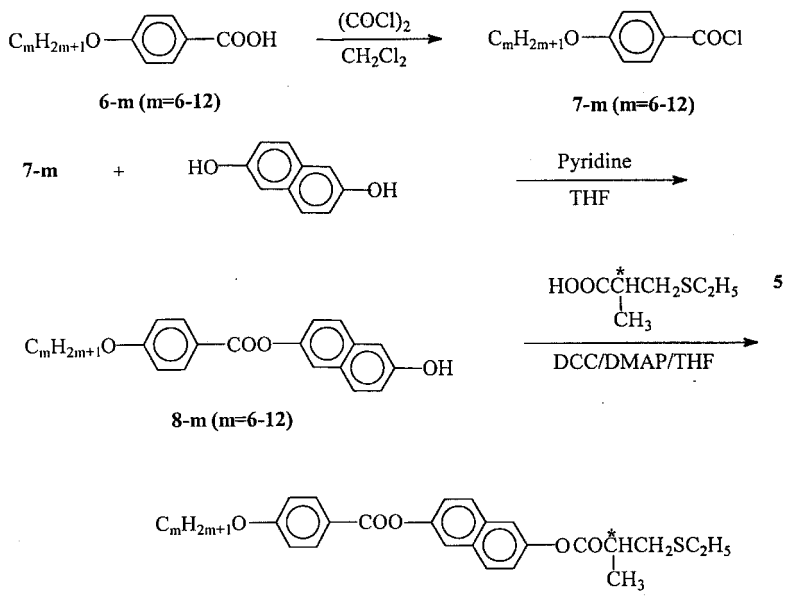

Scheme 2. The synthetic procedures for the chiral materials EMMPN*m*B (*m* = 6–12).

The detailed synthetic procedures and results are described below.

2.2.1. *(R)- and (S)-3-Ethylmercapto-2-methylpropionic acid,* ***5a*** *and* ***5b***

For the (*R*)-enantiomer, the specific rotation is $[\alpha]_D^{22} = +26.45$ (C 2.00, $CHCl_3$). Elemental analysis: calculated for $C_6H_{12}O_2S_1$, C 48.62, H 8.16; found, C 48.57, H 8.08%. Chemical shifts of compound **5a** in ^{1}H NMR (400 MHz, $CDCl_3$): δ (ppm) 1.18 (t, 3H, J = 7.4 Hz), 1.22 (d, 3H, J = 6.8 Hz), 2.49 (q, 2H, J = 7.2 Hz), 2.52 (dd, 1H, J = 6.9, 12.7 Hz), 2.59–2.66 (m, 1H), 2.79 (dd, 1H, J = 6.9, 12.7 Hz), 10.60 (br, 1H). For the (*S*)-enantiomer, the specific rotation is $[\alpha]_D^{22} = \pm 26.39$ (C 2.00, $CHCl_3$). Elemental analysis: calculated for $C_6H_{12}O_2S_1$, C 48.62, H 8.16; found, C 48.65, H 8.10%. Chemical shifts of compounds **5b** in ^{1}H NMR (400 MHz, $CDCl_3$): δ (ppm) 1.18 (t, 3H, J = 7.4 Hz), 1.22 (d, 3H, J = 6.8 Hz), 2.49 (q, 2H, J = 7.2 Hz), 2.52 (dd, 1H, J = 6.9, 12.7 Hz), 2.59–2.66 (m, 1H), 2.79 (dd, 1H, J = 6.9, 12.7 Hz), 10.60 (br, 1H).

2.2.2. *4-Alkoxybenzoic acid chloride,* ***7-m*** *(**m** = 6–12)*

4-Alkoxybenzoic acids (6 mmol) were reacted with oxalyl chloride (2.66 mmol) in CH_2Cl_2 (6 ml) at reflux temperature for 2 h under nitrogen. After excess oxalyl chloride was completely removed, the precipitates were used immediately for the ensuing reactions.

2.2.3. *6-Hydroxynaphth-2-yl 4-alkoxybenzoates,* ***8-m*** *(**m** = 6–12)*

Compound **7-m** (6 mmol) dissolved in CH_2CI_2 was added dropwise to a mixture of 2,6-dihydroxynaphthalene (30 mmol), dried pyridine (5 ml) and anhydrous THF (30 ml). The reaction mixture was cooled in refrigerator for 2 days. Silica gel was then added and the mixture was dried and powdered. The product was collected by column chromatography over silica gel (70–230 mesh) using dichloromethane as eluent. White precipitates in 40–50% yields were obtained after recrystallization from absolute ethanol. The results of elemental analysis, for an example of compound **8-*m*** (***m*** = **10**): calculated for $C_{12}H_{32}O_4$, C 77.1 1, H 7.67; found, C 77.08, H 7.69%. Chemical shifts of **8-*m*** (***m*** = **10**) in ^{1}H NMR (400 MHz, $CDCl_3$): δ (ppm) 0.8 (t, 3H), 1.2–1.8 (m, 12H), 4.05 (t, 2H), 5.6 (s, 1H), 6.97–6.99 (dd, 4H, J = 8 Hz), 7.25 (s, 1H), 7.53–7.59 (m, 3H, J = 8 Hz), 8.17–8.19 (dd, 2H, J = 8 Hz).

2.2.4. *(R)- and (S)-6-(3-Ethylmercapto-2-methylpropionyloxy)-2-naphthyl 4-alkoxybenzoates, (R)- and (S)-EMMPNmB (**m** = 6–12)*

A mixture of compound **8** (1.49 mmol), compound **5** (0.2 g, 1.35 mmol), DCC (0.389 g, 1.89 mmol), DMAP (0.0165 g, 0.135 mmol) and anhydrous THF (6 ml) was stirred at room temperature for 2 days. After work-up procedure, the product was isolated by silica gel (70–230 mesh) column chromatography using CH_2Cl_2 as eluent

and then purified by recrystallization from absolute ethanol. White precipitates in 70–75% yields were obtained. The molecular structure and purity of the target materials were identified and analysed by ^{1}H NMR spectroscopy and elemental analysis. Typical example of chemical shifts for compound (*R*)EMMPN10B in ^{1}H NMR (400 MHz, $CDCl_3$): δ (ppm) 0.8–1.8 (m, 25H), 2.5 (q, 2H), 2.52 (dd, 1H), 2.6–2.68 (m, 1H), 2.79 (dd, 1H), 4.0 (t, 2H), 6.9–7.0 (dd, 4H), 7.2 (s, 1H), 7.5–7.6 (m, 3H), 8.2–8.3 (dd, 2H). The results of elemental analysis and the specific rotations $[\alpha]_D$ of the target materials are listed in Table 1.

3. Results and discussion

3.1. *Thermal optical microscopic investigations*

Samples mounted between two untreated glass slides were used for thermal optical observations. As an example, on cooling compound (*R*)-EMMPN10B from the isotropic liquid (I), a blue phase (BP) was formed as characterized by formation of grazed platelet texture, figure 1 (*a*). This was followed by the formation of a paramorphotic defective texture, figure 1 (*b*), indicating a growth of the chiral nematic (N*) phase. On further cooling, a texture of spiral filaments, figure 1 (*c*) appeared and was identified by the characteristics of twisted grand boundary A* (TGB_A^*) phase [14, 15]. This phase, detected in a 5 µm thick homogeneously aligned cell, displayed a kind of Grandjean texture similar to that observed for the cholesteric phase [6, 16, 17]. As the temperature continued to fall, the texture displayed declination lines on the filament domain preserved from the virtual TGB_A phase, figure 1 (*d*) and was characterized as the existence of twisted grand boundary C* (TGB_C^*) phase [9, 14].

In a study of the racemic modification of compound (±)-EMMPN10B, a 1:1 (by weight) mixture of compounds (*R*)-EMMPN10B and (*S*)-EMMPN10B, displayed normal nematic (N), smectic A (SmA),

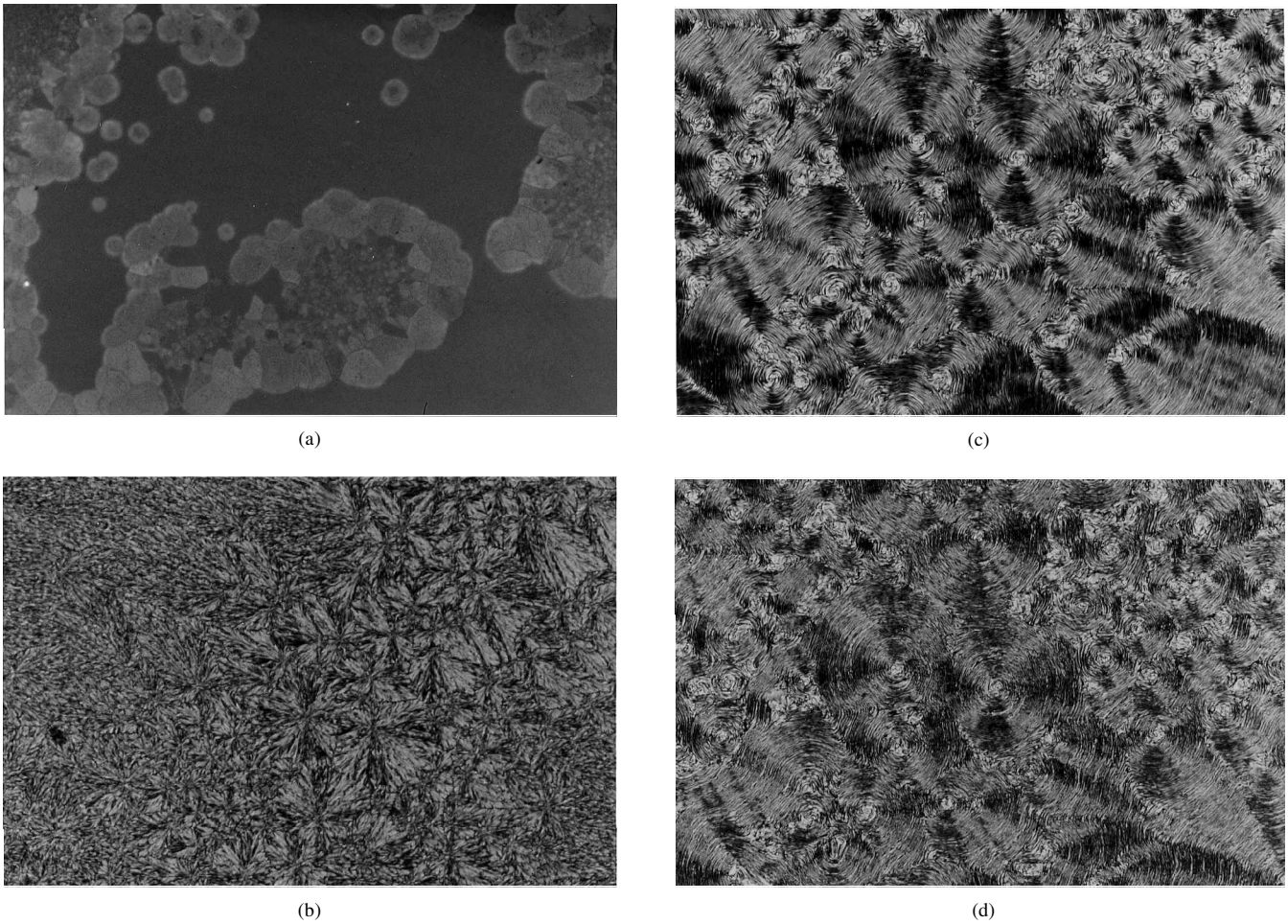

Figure 1. Microphotographic textures of the mesomorphic phases obtained from (R)-EMMPN10B: (a) the grazed platelet texture of the blue phase, (b) the paramorphotic defect texture of the N* phase, (c) the spiral filament texture of the TGB_A^* phase, and (d) the spiral filament texture with declination lines of the TGB_C^* phase.

Table 1. Results of analysis and specific rotation $[\alpha]_D$ for compounds (*R*)- and (*S*)-EMMPN*m*B.

Compound	Elemental analysis/%	C	H	$[\alpha]_D^{26}$ (conc/g per 100 ml)[a]
(*R*)-EMMPN6B	Calcd.	70.42	6.93	+ 43.2(0.606)
	Found	70.41	6.92	
(*R*)-EMMPN7B	Calcd.	70.83	7.14	+ 35.5(0.602)
	Found	70.80	7.11	
(*R*)-EMMPN8B	Calcd.	71.23	7.33	+ 38.4(0.606)
	Found	71.20	7.25	
(*R*)-EMMPN9B	Calcd.	71.61	7.52	+ 33.6(0.597)
	Found	71.47	7.53	
(*R*)-EMMPN10B	Calcd.	71.96	7.69	+ 39.0(0.603)
	Found	71.95	7.71	
(*S*)-EMMPN10B	Calcd.	71.96	7.69	− 38.7(0.605)
	Found	71.95	7.71	
(*R*)-EMMPN11B	Calcd.	72.30	7.86	+ 37.4(0.612)
	Found	72.20	7.85	
(*R*)-EMMPN12B	Calcd.	72.63	8.02	+ 30.4(0.601)
	Found	72.58	8.04	

[a] Solvent: dichloromethane.

and smectic C (SmC) phases in the cooling process. The phase sequence of I–BP–N*–TGB_A^*–TGB_C^* in the enantiomers became that of I–N–SmA–SmC in racemic texture. Surprisingly, it was found that the SmA phase is enantiotropic in the racemic mixture unlike the TGB_A^* phase, which is monotropic in the enantiomers. This phenomenon suggests that the chirality of this molecule could suppress the formation of smectic phase in the heating process. It also implies that these chiral materials have such a high chirality that the twisting power of the helix overrides the ease of smectic layer packing, and results in a disappearance of the SmA* phase, and formation of the TGB_A^* phase in the heating stage.

The mesophases of enantiomers and racemic mixtures, and their corresponding transition temperatures determined by thermal optical microscopy, are summarized in table 2. The phase diagram plotted as a function of increasing terminal alkyl chain length, *m*, in the cooling process is presented in figure 2. It can be seen that the compound of $m = 7$ is not mesogenic, and that of $m = 6$ shows monotropic BP and N* phases. Increasing *m* favours the formation of TGB phases; in particular, when *m* is greater than 11, both TGB_A^* and TGB_C^* phases become enantiotropic. The I–BP, BP–N* and N*–TGB_A^* phase transition temperatures display an odd–even effect and gradually rise as *m* increases. The thermal stability of the TGB_A^* phase is greatest at $m = 8$ and 9, and reduces as *m* increases; whereas that of the TGB_C^* phase increases as $m \geqq 10$. Increasing *m* favours the formation of the TGB phases, with an accompanying change from monotropic to enantiotropic phases.

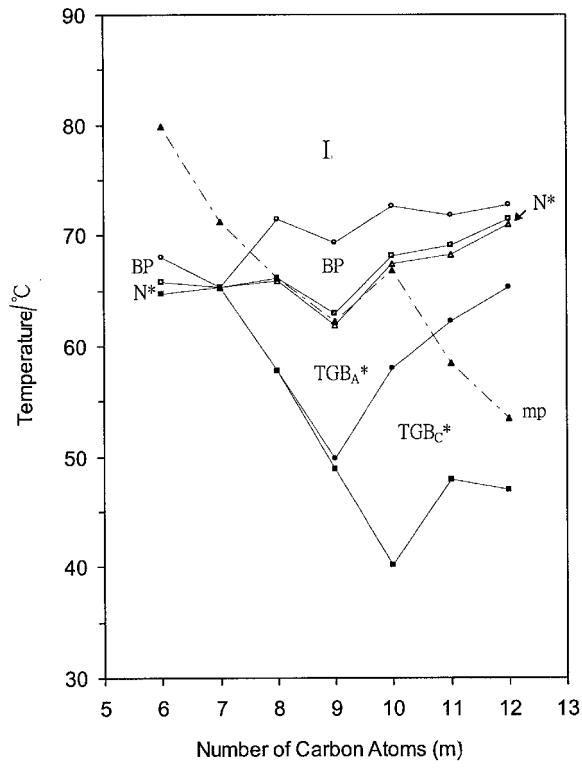

Figure 2. A plot of transition temperatures as a function of the alkyl chain length, m, for compounds EMMPNmB ($m = 6$–12). The mesophases of each compound which only appear at temperatures below melting point indicate that the mesophases are monotropic otherwise enantiotropic. (○) Iso-Bp transition; ( ) BP-N* transition, (Δ) N*-TGB_A^* transition; (●) TGB_A^*-Cr or TGB_A^*-TGB_C^* transition; (■) N*-Cr, TGB_A^*-Cr or TGB_C^*-Cr transition; (▲) melting point, mp.

Surprisingly, it can be seen that the N* phase behaves as an intermediary phase between BP and TGB_A^* phases in rather narrow temperature ranges (calc. 0.5–1.4°C). This phenomenon strongly suggests that these chiral materials have a tendency to generate frustrated phases.

3.2. *Calorimetric study*

The DSC thermograms were recorded using a DuPont DSC-910 calorimeter with heating and cooling rates of 1°C min^{-1}. The DSC thermal traces obtained from the enantiomers and their racemic modifications are shown in figure 3. For the enantiomers, the DSC traces show that the crystal (Cr) melts to BP phase, and subsequently to isotropic liquid in the heating cycle. However, three phase transitions, I–BP, N*–TGB_A^* and TGB_C^*–Cr, appear significantly in the cooling cycle, indicating that N*, TGB_A^* and TGB_C^* phases are monotropic. The transition peaks of the BP–N* and N*–TGB_A^* transitions are overlapped; the enthalpies of these transitions are summed and listed in table 2. The enthalpy of the

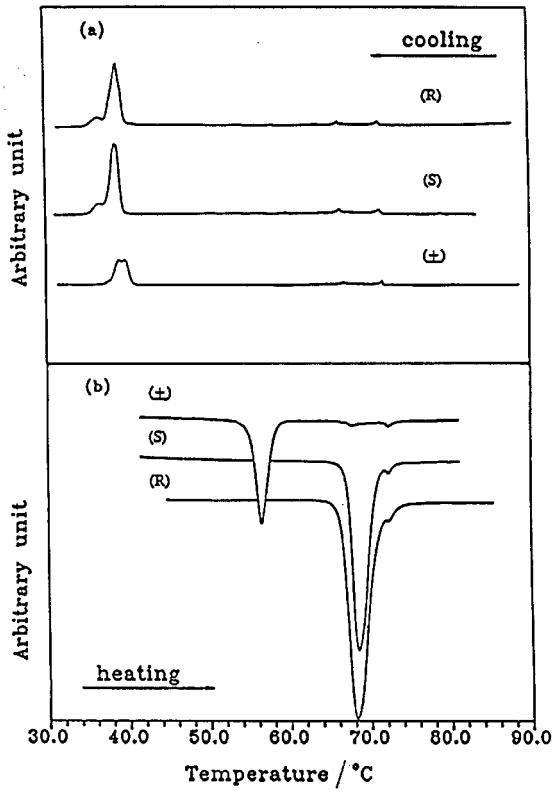

Figure 3. Heating and cooling thermograms for compounds EMMPN10B. The heating and cooling rate was 1°C min^{-1}.

TGB_A^*–TGB_C^* transition cannot be measured by the calorimetric method. The racemic mixture (±)-EMMON10B exhibits Cr–SmA, SmA–N and N–I phase transitions. The SmA–SmC transition also cannot be detected by the calorimetric method. The temperature of clearing points in the racemic mixture is considerably higher (calc. 0.3–0.4°C) than that in the enantiomers. A similar trend is also detected in the temperatures of the N–SmA transition relative to that of the N*–TGB_A^* transition. However, an opposite result appears in the temperatures of the SmA–SmC transition with respect to that of TGB_A^*–TGB_C^* transition. The enthalpies of the clearing points (I–BP transitions) sharply fall as the terminal chain length *m* is decreased. Thus, transitions of the clearing points appear to become more weakly first order in nature with decreasing *m*.

3.3. *Physical properties*

Samples filled in 5 μm homogeneously aligned cells were used for the measurement of physical properties. A frequency alternating electric field (20 V) was applied to the cells to manipulate the cell sample into a form of unit domain. Consequently, the TGB_A^* and TGB_C^* phases in these cells were surface stabilized, resulting in a structural geometry similar to that obtained from the materials possessing SmA* and ferroelectric SmC*

Table 2. Transition temperatures (°C) and enthalpies (J g^{-1}) of phase change for the compounds (*R*)- and (*S*)-EMMPN*m*B; () refer to monotropic phase.

Compound	I		BP		N*/N		TGB_A^*/SmA		TGB_C^*/SmC		Cr	m.p.
(*R*)-EMMPN6B	•	(68.0)	•	(65.8)	•		—		—	(64.7)	•	79.9
Δ*H*		0.12		6.52						17.34		
(*R*)-EMMPN7B	•		—		—		—		—	65.3	•	71.2
Δ*H*										32.55		
(*R*)-EMMPN8B	•	71.4	•	(66.1)	•	(65.9)	•		—	(57.7)	•	66.2
Δ*H*		0.33				0.71[a]				25.15		
(*R*)-EMMPN9B	•	69.3	•	63.0	•	(61.9)	•	(49.8)[b]	•	(48.9)	•	62.3
Δ*H*		0.38				0.54[a]		—[c]		26.36		
(*R*)-EMMPN10B	•	72.6	•	68.2	•	(67.4)	•	(58.0)[b]	•	(40.2)	•	66.8
Δ*H*		0.47				0.51[a]		—[c]		18.49		
(*S*)-EMMPN10B	•	72.3	•	68.1	•	(67.3)	•	(57.8)[b]	•	(40.1)	•	67.1
Δ*H*		0.44				0.52[a]		—[c]		18.90		
(±)-EMMPN10B	•		—	72.7	•	67.9	•	57.5[b]	•	(36.4)	•	55.0
Δ*H*				0.49		0.38		—[c]		15.40		
(*R*)-EMMPN11B	•	71.8	•	69.1	•	68.3	•	62.2[b]	•	(47.9)	•	58.5
Δ*H*		1.03				1.08[a]		—[c]		22.38		
(*R*)-EMMPN12B	•	72.8	•	71.50	•	71.0	•	65.3[b]	•	47.0	•	53.5
Δ*H*		1.34				1.31[a]		—[c]		23.00		

[a] Δ*H* (BP–N*–TGB_A^*).
[b] The temperatures were determined by optical microscopy.
[c] The enthalpies were too small to be measured.

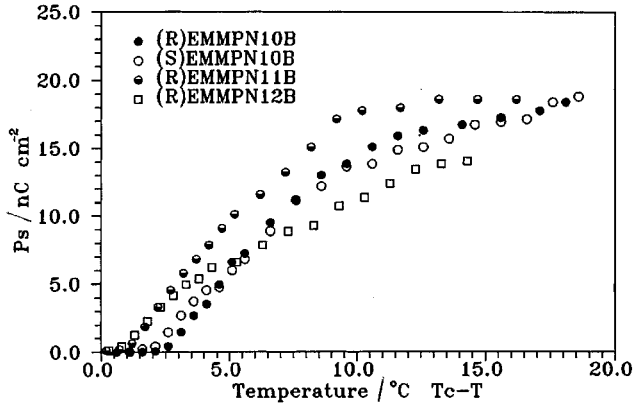

Figure 4. Spontaneous polarization as a function of temperature for compounds EMMPN*m*B (*m* = 10–12).

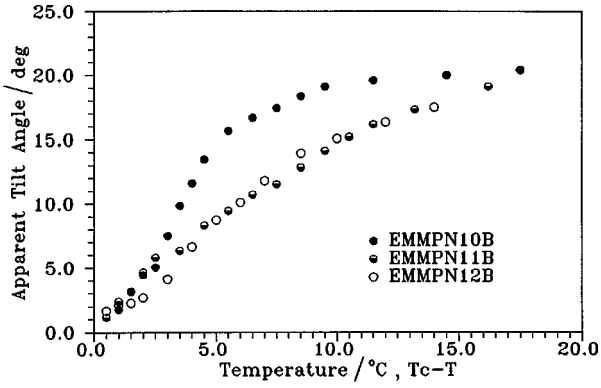

Figure 5. Temperature dependence of apparent tilt angles for compounds EMMPN*m*B (*m* = 10–12); applied voltage = 20.0 V.

phases [9]. These materials in surface stabilized geometry were then used for the measurement of physical properties.

Figure 4 presents the magnitude of spontaneous polarization $\mathbf{P}_S$ as a function of temperature for compounds EMMPN*m*B (*m* = 10–12). It indicates that the order of magnitudes for $\mathbf{P}_S$ values are moderate (calc. 14–19 nC cm^{-2}). Moreover, the $\mathbf{P}_S$ values of enantiomers are nearly the same at any temperature below the Curie point (T_C). Figure 5 shows that the tilt angles are small at the SmA*–SmC* phase transition and then increase drastically as the temperature cools below the Curie point. The maximum apparent tilt angle is about 20°.

4. Conclusions

A new homologous series of chiral materials, (*R*)- and (*S*)-EMMPN*m*B (*m* = 6–12), derived from (*R*)- and (*S*)-3-ethylmercapto-2-methylpropionic acids, has been synthesized. The compounds, with the exception of EMMPN6B, are mesogenic. These chiral materials display mostly stable frustrated BP, TGB_A^* and TGB_C^* phases; the N* phase exists as an intermediary phase in the transformation from BP to TGB_A^*. It is thus considered that these materials may provide a better structural model for future studies on the appearance of frustrated phases.

References

[1] Coates, D., and Gray, G. W., 1973, *Phys. Lett.*, **45A,** 115.
[2] Armitage, D., and Price, F. P., 1876, *J. appl. Phys.*, **47,** 2735.
[3] Stegemeyer, H., Blumel, T. H., Hiltrop, K., Onusseit, H., and Porsch, F., 1986, *Liq. Cryst.*, **1,** 3.
[4] Crooker, P. P., 1989, *Liq. Cryst.*, **5,** 751.
[5] Goodby, J. W., Waugh, M. A., Stein, S. M., Chin, E., Pindak, R., and Patel, J. S., 1989, *Nature*, **337,** 449.
[6] Goodby, J. W., Waugh, M. A., Stein, S. M., Chin, E., Pindak, R., and Patel, J. S., 1989, *J. Am. chem. Soc.*, **111,** 8119.
[7] Nguyen, H. T., Bouchta, A., Navailles, L., Barois, P., Isaert, N., Twieg, R. J., Maroufi, A., and Destrade, C., 1992, *J. Phys. II (Fr).*, **2,** 1889.
[8] Shao, R. F., Pang, J. H., Clark, N. A., Rego, J. A., and Walba, D. M., 1993, *Ferroelectrics*, **147,** 255.
[9] Slaney, A. J., and Goodby, J. W., 1991, *J. mater. Chem.*, **1,** 5.
[10] Booth, C. J., Dunmur, D. A., Goodby, J. W., Kang, J. S., and Toyne, K. J., 1994, *J. mater. Chem.*, **4,** 747.
[11] Goodby, J. W., Slaney, A. J., Booth, C. J., Nishyama, I., Yuijk, J. D., Styrng, P., and Toyne, K. J., 1994, *Mol. Cryst. liq. Cryst.*, **243,** 231.
[12] Wu, S. L., Huang, F. K., Uang, B. J., and Tsai, W. J., 1995, *Liq. Cryst.*, **18,** 715.
[13] Miyasato, K., 1983, *Jpn. J. appl. Phys.*, **22,** L661.
[14] Wu, S. L., and Hsieh, W. J., 1996, *Liq. Cryst.*, **21,** 783.
[15] Kuczynski, W., and Stegemeyer, H., 1994, *Ber. Bunsenges phys. Chem.*, **98,** 1322.
[16] Grandjean, M. F., 1921, *C. R. Acad. Sci.*, **172,** 71.
[17] Dierkine, I., and Lagerwall, S. T., 1999, *Liq. Cryst.*, **26,** 83.